

Gravitational Waves Induced by Scalar Perturbations with a Lognormal Peak

Shi Pi^{a,b}, and Misao Sasaki^{a,c,d}

^a *Kavli Institute for the Physics and Mathematics of the Universe (WPI), Chiba 277-8583, Japan*

^b *CAS Key Laboratory of Theoretical Physics, Institute of Theoretical Physics,
Chinese Academy of Sciences, Beijing 100190, China*

^c *Yukawa Institute for Theoretical Physics, Kyoto University, Kyoto 606-8502, Japan*

^d *Leung Center for Cosmology and Particle Astrophysics,
National Taiwan University, Taipei 10617*

(Dated: August 27, 2020)

We study the stochastic gravitational wave (GW) background induced by the primordial scalar perturbation with the spectrum having a lognormal peak of width Δ at $k = k_*$. We derive an analytical formula for the GW spectrum Ω_{GW} for both narrow ($\Delta \ll 1$) and broad ($\Delta \gtrsim 1$) peaks. In the narrow-peak case, the spectrum has a double peak feature with the sharper peak at $k = 2k_*/\sqrt{3}$. On the infrared (IR) side of the spectrum, we find power-law behavior with a break at $k = k_b$ in the power-law index where it changes from k^3 on the far IR side to k^2 on the near IR side. We find the ratio of the break frequency to the peak frequency is determined by Δ as $f_b/f_p \approx \sqrt{3}\Delta$, where f_b and f_p are the break and peak frequencies, respectively. In the broad-peak case, we find the GW spectrum also has a lognormal peak at $k = k_*$ but with a smaller width of $\Delta/\sqrt{2}$. Using these derived analytic formulae, we also present expressions for the maximum values of Ω_{GW} for both narrow and broad cases. Our results will provide a useful tool in searching for the induced GW signals in the coming decades.

PACS numbers:

I. INTRODUCTION

The detection of gravitational waves (GWs) from the mergers of black holes (BHs) and neutron stars by LIGO/Virgo [1] has marked the beginning of the era of gravitational wave astronomy. Besides GW bursts from mergers, there are also stochastic backgrounds of various origins such as GWs from binary inspirals, GWs from first order phase transitions in the early universe, primordial GWs from inflation, and the induced GWs from the primordial scalar perturbation. In the spatially homogeneous and isotropic background, the tensor and scalar perturbations are decoupled at linear order, but they are coupled to each other at nonlinear order [2], giving rise to the induced GWs or secondary GWs [3–28]. The primordial scalar perturbation (more precisely scalar-type curvature perturbation) produces the cosmic microwave background radiation (CMB) anisotropy and seeds the large scale structure of the universe, and its properties are tightly constrained observations. Namely, it is Gaussian with a nearly scale-invariant spectrum with the rms amplitude of 10^{-5} on scales larger than around 1 Mpc [29]. The GWs induced by such primordial scalar perturbation is also nearly scale-invariant at frequencies higher than 10^{-15} Hz, but the amplitude is negligibly small to be detected [3], and perhaps smaller than GWs from the primordial tensor perturbation [30, 31].

However, on scales much smaller than 1 Mpc, the amplitude of the primordial scalar perturbation is only weakly constrained, and hence it is possible to be large [32–34]. An interesting consequence associated with a large scalar perturbation is the formation of primordial black holes (PBHs). If the rms scalar perturbation amplitude is large at some specific wavenumber, PBHs can form from the high σ peaks when the corresponding wavelengths reenter the Hubble horizon [35, 36]. The current observational constraints does not exclude the existence of a substantial amount of such PBHs. There are actually several interesting “mass windows” [37], which can lead to fruitful phenomena. For instance, the detection of GWs by LIGO/Virgo has revealed the ubiquitous existence of BHs with $10 \sim 100M_{\odot}$, which revives our interest in the hypothesis that such BH binaries are formed by PBHs [38]. It is also probable that PBHs are the dominant component of the dark matter if they are in the mass range $10^{19} \sim 10^{22}$ g, which avoids recent observational constraints [39]. In addition, PBHs may seed the galaxy or structure formation [40], the planet 9 [41], or they may provide a mechanism for baryogenesis [42]. For review of PBHs and their observational constraints, see [43, 44].

To generate an amount of PBHs comparable to the energy density of cold dark matter, the spectrum of the primordial scalar perturbation is required to have an amplitude of order 10^{-2} . Such a spectrum with a high peak can be realized in various models of inflation, for instance, models with potential having a near-inflection point [45–55], modified

gravity [56–63], multi-field inflation [64–74], curvaton scenarios [75–78], models with parametric resonance [79–83], etc.. The induced GWs from these models may be detected in the near future by the current and future detectors like LIGO/Virgo, KAGRA [84], LISA [85], Taiji [86], Tianqin [87], ET [88], DECIGO [89], BBO [90], FAST [91], and SKA [92]. The peak frequency of the induced GWs is related to the associated PBH mass as $f_{\text{peak}} = 6.7 \times 10^{-9} (M_{\text{PBH}}/M_{\odot})^{-1/2}$ Hz [6]. If LIGO detections are PBHs, the induced GWs peak at nHz, right in the detection range of pulsar timing array (PTA) [93]. The fact that there is no detection at present has already started to constrain the PBHs-as-LIGO-BHs scenario [94]. For asteroid-mass PBHs, the associated induced GWs peak at $\sim 10^{-3}$ Hz, which must be detectable by LISA if PBHs are the dark matter [18].

The spectrum of the induced GWs from a δ -function peak of the scalar perturbation was studied in Refs. [4, 6, 12, 13], and an analytical expression for the GW spectrum was derived in Ref. [17]. However, it was found that the infrared scaling of the GW spectrum depends sensitively on the width, which is f^2 for a δ -function peak, while f^3 for a finite width, and a transition from f^3 to f^2 was observed for a finite but small width [96, 97]. In the case of a broad peak, the induced GW spectrum was numerically studied and found to have a broad-peak-like feature near its maximum [11, 32, 33]. The goal of this paper is to derive an analytic formula for the induced GW spectrum due to the scalar perturbation with the spectrum having a lognormal peak, for both narrow and broad widths. The result will provide a very useful tool for studying various phenomena associated with the original curvature perturbation.

This paper is organized as follows. In Section II, we collect the necessary formulae needed to calculate the induced GWs. In Section III, we apply the formulae to the curvature perturbation with a lognormal peak. In Section III A and III B, we consider narrow and broad widths and present analytic expressions for the GW spectrum, respectively. We find they agree very well with the numerical results. We summarize our findings in Section IV. As the analytical calculation is a little bit long and tedious, readers may directly go to (19) and (40) to check the main results and Section IV for the conclusions.

II. SETUP

In linear cosmological perturbation, the perturbed metric can be written in the Newton gauge as

$$ds^2 = a^2(\eta) \left[-(1 + 2\Psi)d\eta^2 + ((1 + 2\Phi)\delta_{ij} + h_{ij})dx^i dx^j \right], \quad (1)$$

where Ψ is the Newton potential, Φ is the intrinsic curvature perturbation, and $\Phi = -\Psi$ for negligible anisotropic stress [95], h_{ij} is the transverse traceless (tensor) part of the metric perturbation. In momentum space, the tensor perturbation can be written as

$$h_{ij}(\eta, \mathbf{x}) = \int \frac{d^3k}{(2\pi)^{3/2}} \sum_{\lambda=+, \times} e_{ij}^{\lambda}(\hat{k}) h_{\mathbf{k}, \lambda}(\eta) e^{i\mathbf{k} \cdot \mathbf{x}}, \quad (2)$$

where $e_{ij}^{\lambda}(\hat{k})$ are two orthonormal polarization tensors perpendicular to \hat{k} -direction. The equation of motion for the tensor perturbation of each polarization at second order is sourced by the scalar perturbation:

$$h''_{\mathbf{k}, \lambda} + 2\mathcal{H}h'_{\mathbf{k}, \lambda} + k^2 h_{\mathbf{k}, \lambda} = \mathcal{S}_{\lambda}(\mathbf{k}, \eta) = \int d^3\ell e_{ij}^{\lambda}(\mathbf{k}) q^i q^j f(\mathbf{k}, \boldsymbol{\ell}, \eta) \Psi_{\boldsymbol{\ell}} \Psi_{\mathbf{k}-\boldsymbol{\ell}}, \quad (3)$$

where the source term, $\mathcal{S}_{\lambda}(\mathbf{k}, \eta)$, is the convolution of the scalar perturbation, which can be factorized into the primordial part $\psi_{\boldsymbol{\ell}} \psi_{\mathbf{k}-\boldsymbol{\ell}}$ and the combination of the transfer function $T(\ell, \eta)$:

$$f(\mathbf{k}, \boldsymbol{\ell}, \eta) = 6T(|\mathbf{k} - \boldsymbol{\ell}| \eta) T(\ell \eta) + 3\eta \frac{\partial T(|\mathbf{k} - \boldsymbol{\ell}| \eta)}{\partial \eta} T(\ell \eta) + 2\eta^2 \frac{\partial T(|\mathbf{k} - \boldsymbol{\ell}| \eta)}{\partial \eta} \frac{\partial T(\ell \eta)}{\partial \eta}; \quad \Psi(\mathbf{k}, \eta) = T(k\eta) \psi_{\mathbf{k}}. \quad (4)$$

In this paper we only consider the wavenumbers that reenter the Hubble horizon during the radiation-dominated stage. For the case of an (early) matter-dominated stage, see Refs. [7, 17, 24–26, 28], while for an arbitrary background, see Refs. [99, 100] and a companion paper [101]. The power spectra of the primordial scalar perturbation and the tensor perturbation are defined as

$$\begin{aligned} \langle \psi_{\mathbf{k}} \psi_{\mathbf{q}} \rangle &= \frac{2\pi^2}{k^3} \mathcal{P}_{\psi}(k) \delta^{(3)}(\mathbf{k} + \mathbf{p}). \\ \sum_{\lambda=+, \times} \langle e_{ij}^{\lambda} e_{\lambda}^{ij} h_{\mathbf{k}, \lambda}(\eta) h_{\mathbf{p}, \lambda}(\eta) \rangle &= \frac{2\pi^2}{k^3} \mathcal{P}_h(k, \eta) \delta^{(3)}(\mathbf{k} + \mathbf{p}). \end{aligned} \quad (5)$$

The power spectrum of the primordial Newton potential is related to that of the conserved comoving curvature perturbation in the radiation dominated universe as $\mathcal{P}_\psi = (4/9)\mathcal{P}_\mathcal{R}$. As mentioned in Introduction, the constraint by Planck is $\mathcal{P}_\mathcal{R}(k) \approx 2.1 \times 10^{-9}$ at $k = 0.05 \text{ Mpc}^{-1}$ [29]. However, since the scales we have in mind are substantially smaller than 1 Mpc, we are free from the Planck constraint. We will specify the form of $\mathcal{P}_\mathcal{R}(k)$ on small scales later.

The equation of motion for $h_{\mathbf{k}}$ can be solved by the Green function method. In the radiation-dominated universe,

$$h_{\mathbf{k},\lambda}(\eta) = \int_{\eta_0}^{\eta} d\tilde{\eta} \frac{\sin k(\eta - \tilde{\eta})}{k} \frac{a(\tilde{\eta})}{a(\eta)} \mathcal{S}(\mathbf{k}, \tilde{\eta}). \quad (7)$$

The two-point correlation function of the tensor perturbation is given by

$$\begin{aligned} \langle h_{\mathbf{k},\lambda}(\eta) h_{\mathbf{p},\lambda'}(\eta) \rangle &= \delta_{\lambda,\lambda'} \int_{\eta_0}^{\eta} d\eta_2 \int_{\eta_0}^{\eta} d\eta_1 \frac{a(\eta_2)}{a(\eta)} \frac{a(\eta_1)}{a(\eta)} \frac{\sin k(\eta - \eta_1)}{k} \frac{\sin p(\eta - \eta_2)}{p} f(\mathbf{k}, \boldsymbol{\ell}, \eta_1) f(\mathbf{p}, \mathbf{q}, \eta_2) \\ &\times \left(\frac{4}{9}\right)^2 8\pi^4 \int \frac{d^3\ell}{(2\pi)^{3/2}} e_{ij}^{\lambda}(\hat{k}) \ell^i \ell^j \int \frac{d^3q}{(2\pi)^{3/2}} e_{lm}^{\lambda'}(\hat{p}) q^l q^m \frac{\mathcal{P}_\mathcal{R}(\ell) \mathcal{P}_\mathcal{R}(|\mathbf{k} - \boldsymbol{\ell}|)}{\ell^3 |\mathbf{k} - \boldsymbol{\ell}|^3} \delta^{(3)}(\mathbf{k} + \mathbf{p}) \delta^{(3)}(\boldsymbol{\ell} + \mathbf{q}). \end{aligned} \quad (8)$$

Here it may be worth mentioning that we do not assume anything about the statistical nature of the primordial scalar perturbation. It may be Gaussian or may be highly non-Gaussian. The essential point is that the spectrum of the induced GWs is given by a convolution of the primordial curvature perturbation spectrum, independent of its statistical nature. Nevertheless, we also mention that it may be possible to obtain the information about the non-Gaussianity if we combine the predictions on the induced GWs and those on the corresponding abundance of PBHs [18].

Cosmologists commonly call the GW energy density per logarithmic interval of wavenumber, normalized by the total energy density of the universe as the GW spectrum,

$$\Omega_{\text{GW}}(k, \eta) = \frac{1}{\rho_{\text{tot}}} \frac{d\rho_{\text{GW}}}{d \ln k} = \frac{k^2}{12H^2 a^2} \mathcal{P}_h(k, \eta). \quad (9)$$

The power spectrum of the tensor perturbation is defined in (6) by the 2-point correlation function, which is expressed in (8). To step further we have to calculate the time integral of the transfer functions, and average it over many oscillating periods, which is done in Refs. [16, 17, 26]. Following Ref. [17], we define a set of new variables, $u = |\mathbf{k} - \boldsymbol{\ell}|/k$, and $v = \ell/k$, and then integrate the solid angular elements perpendicular to $\hat{\ell}$ - and \hat{q} -direction in (8),

$$\begin{aligned} \Omega_{\text{GW},r}(k) &= 3 \int_0^{\infty} dv \int_{|1-v|}^{1+v} du \frac{\mathcal{T}(u, v)}{u^2 v^2} \mathcal{P}_\mathcal{R}(vk) \mathcal{P}_\mathcal{R}(uk), \\ \mathcal{T}(u, v) &= \frac{1}{4} \left[\frac{4v^2 - (1 + v^2 - u^2)^2}{4uv} \right]^2 \left(\frac{u^2 + v^2 - 3}{2uv} \right)^4 \left[\left(\ln \left| \frac{3 - (u+v)^2}{3 - (u-v)^2} \right| - \frac{4uv}{u^2 + v^2 - 3} \right)^2 + \pi^2 \Theta(u + v - \sqrt{3}) \right], \end{aligned} \quad (10)$$

Θ is the step function. The normalization of $\mathcal{T}(u, v)$ is such that when $u \approx v \rightarrow \infty$, we have $\mathcal{T}(u, v) \rightarrow (\ln(u+v))^2/4 \sim (\ln v)^2$. $\Omega_{\text{GW},r}(k)$ in (10) is the spectrum during the radiation dominated era which does not depend on time as it is the asymptotic amplitude averaged over many periods deep inside the horizon. The subscript ‘‘r’’ is added to avoid possible confusion with time-dependent $\Omega_{\text{GW}}(k, \eta)$. This *short wavelength limit* is crucial in the recent discussions on the gauge dependence of the induced GWs [102, 103]. For any form of the power spectrum of the curvature perturbation, the spectrum of the induced GWs in the radiation-dominated stage can be calculated by numerically integrating (10). However, we note that since the GW energy density starts to decay relative to the matter density after the matter-radiation equality, the observational GW spectrum today is given by

$$\Omega_{\text{GW}}(f, \eta_0) h^2 = \frac{g_*(\eta_0)^{4/3}}{g_*(\eta_0) g_{*s}(\eta_k)^{1/3}} \Omega_{r,0} \Omega_{\text{GW},r}(f) = 1.6 \times 10^{-5} \left(\frac{g_{*s}(\eta_k)}{106.75} \right)^{-1/3} \left(\frac{\Omega_{r,0} h^2}{4.1 \times 10^{-5}} \right) \Omega_{\text{GW},r}(f). \quad (11)$$

Here $\Omega_{\text{GW},r}(f)$ is the GW spectrum at matter-radiation equality given by (10), and to compare with the observables we replaced the comoving wavenumber k to the physical frequency f , by $f = k/(2\pi a_0)$. Explicitly, $f = 1.5 \times 10^{-9} (k/1 \text{ pc}^{-1}) \text{ Hz}$.

In the following sections, we calculate $\Omega_{\text{GW},r}$ in (10) for both narrow and broad widths of a lognormal peak in the power spectrum of the primordial curvature perturbation. Comparison of the result with observation signals should be done by using (11) for the current GW spectrum $\Omega_{\text{GW}}(f, \eta_0)$.

III. LOGNORMAL PEAK

In the literature, a lognormal peak in the power spectrum of the curvature perturbation is often considered,

$$\mathcal{P}_{\mathcal{R}}(k) = \frac{\mathcal{A}_{\mathcal{R}}}{\sqrt{2\pi}\Delta} \exp\left(-\frac{\ln^2(k/k_*)}{2\Delta^2}\right), \quad (12)$$

where k_* is the peak wavenumber, Δ is the dimensionless width, and the coefficient is to satisfy the normalization $\int_0^\infty \mathcal{P}_{\mathcal{R}}(k) d\ln k = \mathcal{A}_{\mathcal{R}}$. A lognormal peak in the power spectrum of the primordial curvature perturbation can arise naturally in many inflation models (see below), and it is always a good fit to a peaked spectrum around its peak. Furthermore, the scale-invariant power spectrum responsible for the CMB anisotropies can be included as the infinitely broad limit: $\mathcal{A}_{\mathcal{R}}, \Delta \rightarrow \infty$ while keeping $\mathcal{A}_{\mathcal{R}}/\Delta = \text{constant}$. Another limit is $\Delta \rightarrow 0$, when (12) reduces to the δ -function peak, i.e. $\mathcal{P}_{\mathcal{R}} = \mathcal{A}_{\mathcal{R}}\delta(\ln(k/k_*))$. This is used in some papers of generating PBHs which we will comment more in Sec.III A. For the lognormal peak, (10) reduces to

$$\Omega_{\text{GW},r} = \frac{3}{2\pi} \frac{\mathcal{A}_{\mathcal{R}}^2}{\Delta^2} \int_0^\infty dv \int_{|1-v|}^{1+v} du \frac{\mathcal{T}(u,v)}{u^2 v^2} \exp\left[-\frac{(\ln u)^2 + (\ln v)^2 + 2\ln \kappa \ln(uv) + 2\ln^2 \kappa}{2\Delta^2}\right], \quad (13)$$

where we have defined $\kappa \equiv k/k_*$ for convenience. This GW spectrum is valid until the moment of matter-radiation equality, which is connected to the GW spectrum today by (11).

It is convenient to define the following new variables:

$$s = \frac{1}{\sqrt{2}} \ln(uv), \quad t = \frac{1}{\sqrt{2}} \ln \frac{u}{v}. \quad (14)$$

Under this coordinate transformation, (13) becomes

$$\Omega_{\text{GW},r} = \frac{3}{\pi} \frac{\mathcal{A}_{\mathcal{R}}^2}{\Delta^2} \kappa^2 e^{\Delta^2} \int_{-\infty}^\infty \exp\left[-\frac{(s + \sqrt{2}(\ln \kappa + \Delta^2))^2}{2\Delta^2}\right] ds \int_{\chi(s)}^{\xi(s)} \mathcal{T}(s,t) \exp\left(-\frac{t^2}{2\Delta^2}\right) dt, \quad (15)$$

$$\begin{aligned} \mathcal{T}(s,t) &= \frac{1}{4} \left(\cosh(\sqrt{2}t) - \frac{1}{4} e^{-\sqrt{2}s} - e^{\sqrt{2}s} \sinh^2(\sqrt{2}t) \right)^2 \left(\cosh(\sqrt{2}t) - \frac{3}{2} e^{-\sqrt{2}s} \right)^4 \\ &\times \left\{ \left[\ln \left| \frac{3 - 4e^{\sqrt{2}s} \cosh^2(t/\sqrt{2})}{3 - 4e^{\sqrt{2}s} \sinh^2(t/\sqrt{2})} \right| - \frac{2}{\cosh(\sqrt{2}t) - \frac{3}{2} e^{-\sqrt{2}s}} \right]^2 + \pi^2 \Theta \left(2e^{\frac{s}{\sqrt{2}}} \cosh \frac{t}{\sqrt{2}} - \sqrt{3} \right) \right\}. \end{aligned} \quad (16)$$

The integral on t is bounded by the lines $v = 1 + u$ and $v = |1 - u|$, which correspond to the following curves in the new coordinates,

$$\chi(s) = \mathbf{Re} \left[\sqrt{2} \operatorname{arccosh} \left(\frac{e^{-s/\sqrt{2}}}{2} \right) \right], \quad \xi(s) = \sqrt{2} \operatorname{arcsinh} \left(\frac{e^{-s/\sqrt{2}}}{2} \right), \quad (17)$$

where the real part is taken to ensure that $\chi(s) = 0$ for $s > -\sqrt{2} \ln 2$. The domain is shown in Fig. 1. As the integrand is proportional to Gaussian functions, the result depends crucially on whether the widths of the Gaussian peaks are inside the integration domain or not, which are determined by the values of Δ . We will discuss the cases of $\Delta \ll 1$ and $\Delta \gtrsim 1$ separately in the following subsections.

A. Narrow Peak ($\Delta \ll 1$)

Some models predict a narrow peak in the curvature perturbation, $\Delta \ll 1$ [57, 65, 66, 68, 75, 80–83]. In this case, the main contribution of the integral (15) on s and t comes from the vicinity of the peak, $s = -\sqrt{2}(\ln \kappa + \Delta^2)$ and $t = 0$. For the integral on t in the second line of (15), we can take $t \rightarrow 0$ in $\mathcal{T}(s,t)$, and then perform the Gaussian integral,

$$2 \int_{\chi(s)}^{\xi(s)} \mathcal{T}(s,t) \exp\left(-\frac{t^2}{2\Delta^2}\right) dt \approx \mathcal{T}(s,0) \sqrt{2\pi} \Delta \left[\operatorname{erf} \left(\frac{\xi(s)}{\sqrt{2}\Delta} \right) - \operatorname{erf} \left(\frac{\chi(s)}{\sqrt{2}\Delta} \right) \right]. \quad (18)$$

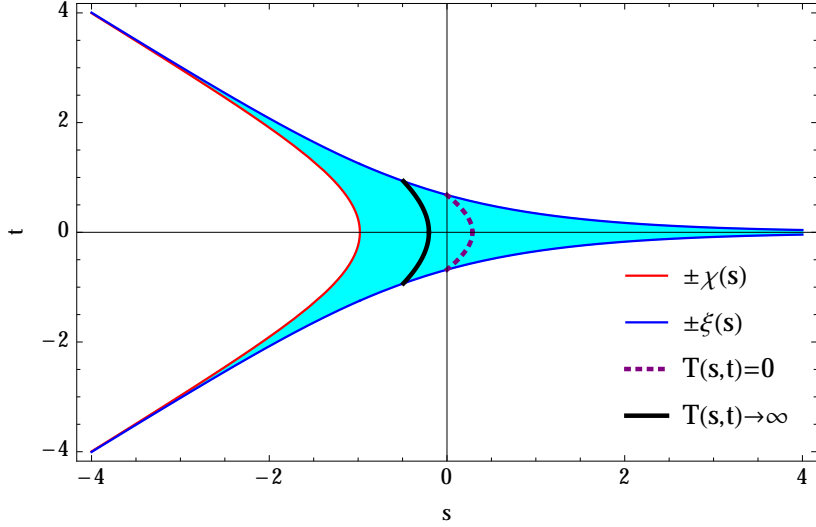


FIG. 1: The shaded area is the domain of integration (15), which is bounded by the curves $\pm\xi(s)$ and $\pm\chi(s)$ shown in (17). We also show the curves of zero points (dotted purple) and the logarithmic divergence (black) in the integral kernel $\mathcal{S}(s, t)$ defined in (16). The former curve is given by $e^{\sqrt{2}s} \cosh(\sqrt{2}t) = 3/2$, while the latter curve is $e^{\sqrt{2}s} \cosh^2(t/\sqrt{2}) = 3/4$.

We substitute this back into (15). Again the narrow Gaussian distribution guarantees that we can take $s \rightarrow -\sqrt{2}(\ln \kappa + \Delta^2)$ in (18), and then perform the Gaussian integral on s . We then obtain an analytical result for the GW spectrum in the narrow-peak case,

$$\Omega_{\text{GW},r} \approx 3\mathcal{A}_{\mathcal{R}}^2 \kappa^2 e^{\Delta^2} \left[\text{erf} \left(\frac{1}{\Delta} \text{arcsinh} \frac{\kappa e^{\Delta^2}}{2} \right) - \text{erf} \left(\frac{1}{\Delta} \text{Re} \left(\text{arccosh} \frac{\kappa e^{\Delta^2}}{2} \right) \right) \right] \left(1 - \frac{1}{4} \kappa^2 e^{2\Delta^2} \right)^2 \left(1 - \frac{3}{2} \kappa^2 e^{2\Delta^2} \right)^2 \cdot \left\{ \left[\frac{1}{2} \left(1 - \frac{3}{2} \kappa^2 e^{2\Delta^2} \right) \ln \left| 1 - \frac{4}{3\kappa^2 e^{2\Delta^2}} \right| - 1 \right]^2 + \frac{\pi^2}{4} \left(1 - \frac{3}{2} \kappa^2 e^{2\Delta^2} \right)^2 \Theta \left(2 - \sqrt{3} \kappa e^{\Delta^2} \right) \right\}, \quad (19)$$

where $\kappa \equiv k/k_*$ as defined before. This analytical result fits quite well with the numerical integration of (13), which is shown in Fig. 2 for $\Delta = 10^{-2}$. In the limit $\Delta \rightarrow 0$, the result reduces to the GW spectrum induced by a δ -function peak, obtained in Ref. [17],

$$\Omega_{\text{GW},r}^{(\delta)} = 3\mathcal{A}_{\mathcal{R}}^2 \kappa^2 \left(1 - \frac{1}{4} \kappa^2 \right)^2 \left(1 - \frac{3}{2} \kappa^2 \right)^4 \left[\left(\frac{1}{2} \ln \left| 1 - \frac{4}{3\kappa^2} \right| - \frac{1}{1 - \frac{3}{2} \kappa^2} \right)^2 + \frac{\pi^2}{4} \Theta \left(2 - \sqrt{3} \kappa \right) \right] \Theta(2 - \kappa). \quad (20)$$

Our narrow-peak result (19) can be further simplified if we approximate $e^{\Delta^2} \approx 1$,

$$\Omega_{\text{GW},r}^{(\Delta \ll 1)} \approx \text{erf} \left(\frac{1}{\Delta} \text{arcsinh} \frac{k}{2k_*} \right) \Omega_{\text{GW},r}^{(\delta)}. \quad (21)$$

We note that the error function factor comes from (18) which is independent of the transfer function (21), implying that this formula is valid for any universe with arbitrary equation of state w . The whole equation-of-state dependence is contained in $\Omega_{\text{GW},r}^{(\delta)}$. In a companion paper [101], an intermediate stage dominated by a scalar field with constant w between inflation and the radiation-dominated universe is considered, where (21) is applied to find the infrared behavior of the induced GWs from a narrow peak.

To summarize, the infrared behavior of GW spectrum is given by (19) or (21) by setting $\kappa \ll 1$,

$$\frac{\Omega_{\text{GW},r}^{(\text{IR})}}{\mathcal{A}_{\mathcal{R}}^2} \approx 3\kappa^2 e^{\Delta^2} \left(\ln \kappa + \Delta^2 \right)^2 \text{erf} \left(\frac{\kappa e^{\Delta^2}}{2\Delta} \right) \approx \begin{cases} 3\kappa^3 \frac{e^{2\Delta^2}}{\sqrt{\pi}\Delta} \left(\ln \kappa + \Delta^2 \right)^2, & \text{for } \kappa < 2\Delta e^{-\Delta^2} \text{ (far-IR);} \\ 3\kappa^2 e^{\Delta^2} \left(\ln \kappa + \Delta^2 \right)^2, & \text{for } 2\Delta e^{-\Delta^2} < \kappa < 1 \text{ (near-IR).} \end{cases} \quad (22)$$

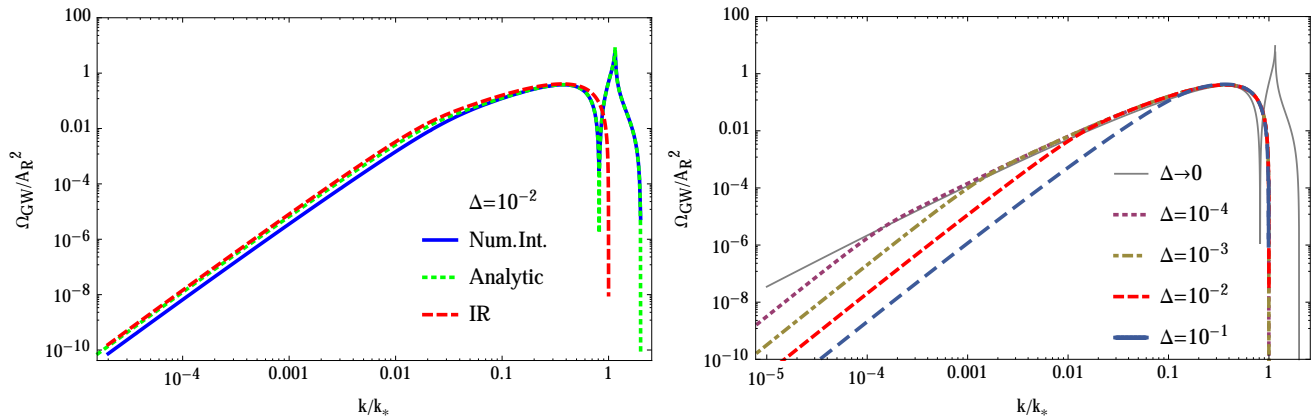


FIG. 2: Left: The GW spectrum with $\Delta = 10^{-2}$. The results of numerical integration of (10), the analytical expression (19), and the infrared approximation (22) are shown. Right: The GW spectra for different values of widths according to the infrared approximation (22). The dashed gray curve is the GW spectrum from a δ -function peak drawn for reference, whose near-peak behavior is nearly the same for all the cases of $\Delta \ll 1$.

In the last step, for an intuitive understanding of the scaling law of the GW spectrum, we use the asymptotic expression for the error function for small and large arguments, respectively, which we refer to as the far-IR and near-IR regions. As clear from the above as well as from Fig. 2, there is a break point at $k/k_* = 2\Delta e^{-\Delta^2}$ where the GW spectrum changes its infrared behavior from $\Omega_{\text{GW},r} \propto k^3$ to $\Omega_{\text{GW},r} \propto k^2$. Let us denote this break wavenumber by k_b , i.e., $k_b = 2\Delta e^{-\Delta^2} k_*$. This feature is characteristic of the GW spectrum induced by a narrowly peaked scalar perturbation, and it is a very useful feature in both identifying the origin of the curvature perturbation and measuring the peak width.

It is clear to see in (19) that besides an infrared local maximum at around $k/k_* = 1/e$, there is another “resonance peak” with logarithmic divergence, which is located at $k = (2/\sqrt{3})e^{-\Delta^2} k_*$, which we denote by k_p . The two maxima are separated by a dip at $k/k_* = \sqrt{2/3}e^{-\Delta^2}$. This two-peak structure is another characteristic feature of the induced GW from a narrow peak, which can be obviously seen for $\Delta \lesssim 0.4$.[§]

The value at the infrared local maximum can be easily estimated as

$$\Omega_{\text{GW},r}^{(\text{IR},\text{max})} \approx \Omega_{\text{GW}} \left(\frac{1}{e} \right) = \frac{3}{e^2} \mathcal{A}_{\mathcal{R}}^2 e^{\Delta^2} (1 - e^2 \Delta^2)^2 \approx 0.41 \mathcal{A}_{\mathcal{R}}^2, \quad (23)$$

where the dependence on the width is of order $\mathcal{O}(\Delta^2)$ and can be neglected. Thus the infrared maximum of $\Omega_{\text{GW},r}$ only depends on the normalization of the curvature perturbation spectrum, which can be clearly seen in the right panel of Fig.2.

As for the resonance peak, it must be smoothed when compared to observation as an infinitely narrow band observation is impossible [104]. For instance, Ref. [32] smooths the resonance peak induced by a δ -function peak on one e -fold. Here we smooth it by taking account of the following fact. For a finite width peak, its width provides a natural smoothing scale,

$$\Omega_{\text{GW},r}^{(\text{res},\text{max})} = \frac{1}{2\Delta} \int_{k_* e^{-\Delta}}^{k_* e^{\Delta}} \Omega_{\text{GW},r} \frac{dk}{k} \approx \frac{4}{9} \mathcal{A}_{\mathcal{R}}^2 \left[(\ln(2\Delta) + 1)^2 + 1 + \frac{\pi^2}{2} \right]. \quad (24)$$

We can see that if Δ is not too small, i.e. for $\Delta \gg (1/2) \exp(-\sqrt{4+2\pi^2} - 1) \approx 0.016$, the smoothed peak value is independent of its width and can be estimated by

$$\Omega_{\text{GW},r}^{(\text{res},\text{max})} \approx \frac{4}{9} \left(1 + \frac{\pi^2}{2} \right) \mathcal{A}_{\mathcal{R}}^2 \approx 2.6 \mathcal{A}_{\mathcal{R}}^2. \quad (25)$$

[§]The origin of the dip and the sharp peak at $k = k_p$ is due to resonance of the tensor modes and scalar modes inside the Hubble horizon due to the difference in their sound speeds [4]. If the sound speeds for both tensor modes and scalar modes are the same, the resonance is absent, and we only have a single smooth peak in the GW spectrum. See Ref. [101].

Note that this is always higher than the infrared peak given in (23). For $\Delta \lesssim 0.016$, the peak is proportional to $(\ln \Delta)^2$, i.e. $\Omega_{\text{GW,r}}^{(\text{res,peak})} \approx (4/9)(\ln \Delta)^2 \mathcal{A}_{\mathcal{R}}^2$. If $f_* \Delta$ is smaller than the frequency resolution, δf , the latter should be used instead as the smoothing scales, though it is unlikely that the observation with such high resolution becomes possible in the near future.

B. Broad Peak ($\Delta \gtrsim \mathcal{O}(1)$)

Many models predict a broad peak in the scalar perturbation, $\Delta \gtrsim \mathcal{O}(1)$ [16, 45–48, 56, 64, 67–70, 74, 76–78]. In this case, we show that the induced GW spectrum has a lognormal peak with width $\Delta/\sqrt{2}$. Since the integrand in (15) is not concentrated around the vicinity of the peak, it is difficult to calculate it at once. It is found that $\mathcal{F}(s, t)$ in the integrand behaves differently for $s \gtrsim 1$, $|s| \sim \mathcal{O}(1)$, and $s \lesssim -1$. We therefore decompose the integral into these three different domains, evaluate each separately, and add up all the contributions at the end to obtain a formula that has sufficiently satisfactory accuracy.

First we consider the domain $s \gtrsim 1$. The contribution in the infrared is mainly from large s , where we may take the leading order of $\mathcal{F}(s, t)$ for $s \gg (1/\sqrt{2}) \ln(3/2)$ as

$$\mathcal{F}(s, t) \approx \frac{s^2}{2} \left[\cosh(\sqrt{2}t) - e^{\sqrt{2}s} \sinh^2(\sqrt{2}t) \right]^2 \cosh^4(\sqrt{2}t). \quad (26)$$

Then since $\xi(s) \ll \Delta$ for $\Delta \gtrsim 1$ and $s \gg 1$, the integral along the t -axis can be approximated by an error function as

$$\int_{-\xi}^{\xi} \mathcal{F}(s, t) \exp\left(-\frac{t^2}{2\Delta^2}\right) dt \approx \frac{8}{15\sqrt{2}} s^2 e^{-s/\sqrt{2}}. \quad (27)$$

Substituting this back into (15), and perform the Gaussian integral along the s -axis, we find

$$\begin{aligned} \Omega_{\text{GW,r}}^{(s \gtrsim 1)} &\approx \frac{4}{5\sqrt{2}\pi} \kappa^3 \frac{e^{9\Delta^2/4}}{\Delta^2} \int_{\frac{1}{\sqrt{2}} \ln \frac{3}{2}}^{\infty} s^2 \exp\left[-\frac{(s + \sqrt{2}(\ln \kappa + \frac{3}{2}\Delta^2))^2}{2\Delta^2}\right] ds, \\ &= \frac{4}{5\sqrt{\pi}} \mathcal{A}_{\mathcal{R}}^2 \kappa^3 \frac{e^{\frac{9\Delta^2}{4}}}{\Delta} \left\{ \left[\left(\ln \kappa + \frac{3}{2}\Delta^2 \right)^2 + \frac{\Delta^2}{2} \right] \text{erfc}\left(\frac{\ln \kappa + \frac{3}{2}\Delta^2 + \frac{1}{2} \ln \frac{3}{2}}{\Delta}\right) \right. \\ &\quad \left. - \frac{\Delta}{\sqrt{\pi}} \exp\left(-\frac{(\ln \kappa + \frac{3}{2}\Delta^2 + \frac{1}{2} \ln \frac{3}{2})^2}{\Delta^2}\right) \left(\ln \kappa + \frac{3}{2}\Delta^2 - \frac{1}{2} \ln \frac{3}{2} \right) \right\}. \end{aligned} \quad (28)$$

where $\text{erfc}(x)$ is the complementary error function defined as $\text{erfc}(x) \equiv 1 - \text{erf}(x)$. For infrared k , $\kappa \ll 1$, the complementary error function approaches 2, while the last term in the curly brackets in (28) is exponentially suppressed. Thus the infrared GW spectrum is given approximately by

$$\Omega_{\text{GW,r}}^{(\text{IR})} \approx \frac{8}{5\sqrt{\pi}} \mathcal{A}_{\mathcal{R}}^2 \frac{e^{\frac{9\Delta^2}{4}}}{\Delta} \kappa^3 \left[\left(\ln \kappa + \frac{3}{2}\Delta^2 \right)^2 + \frac{\Delta^2}{2} \right] \quad \text{for } \kappa \lesssim \sqrt{\frac{2}{3}} \exp\left(-\frac{3}{2}\Delta^2\right). \quad (29)$$

We see the familiar k^3 scaling. On the other hand, for $\kappa \gtrsim \sqrt{\frac{2}{3}} \exp(-\frac{3}{2}\Delta^2)$, the complementary error function is also exponentially suppressed. Taking the large Δ limit of it gives the near-peak behavior,

$$\Omega_{\text{GW,r}}^{(\text{peak}, s \gtrsim 1)} \approx \frac{16 + 24 \ln \frac{3}{2} + 18 \ln^2 \frac{3}{2}}{135\pi} \mathcal{A}_{\mathcal{R}}^2 \frac{e^{9\Delta^2/4}}{\Delta^2} \exp\left(-\frac{(\ln \kappa + \frac{3}{2}\Delta^2 + \frac{1}{2} \ln \frac{3}{2})^2}{\Delta^2}\right). \quad (30)$$

Second, we focus on the domain $|s| \lesssim 1$. There is a discontinuity at $t = \pm\sqrt{2} \text{arccosh}\left(\frac{\sqrt{3}}{2} e^{-s/\sqrt{2}}\right)$ when $|s| \lesssim 1$. The main contribution is from the right hand side of the singularity, as there is an extra π^2 term in the curly brackets in (16), which allows us to take $t \rightarrow 0$ and neglect the logarithm term, giving

$$\mathcal{F}(s, t) \approx \frac{\pi^2}{4} \left(1 - \frac{3}{2} e^{-\sqrt{2}s}\right)^4 \left(1 - \frac{1}{4} e^{-\sqrt{2}s}\right)^2. \quad (31)$$

As this is independent of t , the remaining integral on t is just an error function, which gives

$$\begin{aligned}\Omega_{\text{GW,r}}^{|s|<1} &\approx \frac{3}{\pi} \frac{\mathcal{A}_{\mathcal{R}}^2}{\Delta^2} \kappa^2 e^{\Delta^2} \int_{-\frac{1}{\sqrt{2}} \ln \frac{4}{3}}^{\frac{1}{\sqrt{2}} \ln \frac{3}{2}} ds \exp \left[-\frac{(s + \sqrt{2}(\ln \kappa + \Delta^2))^2}{2\Delta^2} \right] \\ &\quad \times \frac{\pi^2}{4} \left(1 - \frac{3}{2} e^{-\sqrt{2}s}\right)^4 \left(1 - \frac{1}{4} e^{-\sqrt{2}s}\right)^2 \sqrt{\frac{\pi}{2}} \Delta \text{Erf} \left(\frac{\xi(s)}{\sqrt{2}\Delta} \right), \\ &\approx \frac{3\pi}{2\sqrt{2}} \frac{\mathcal{A}_{\mathcal{R}}^2}{\Delta^2} \kappa^2 e^{\Delta^2} \exp \left[-\frac{(\ln \kappa + \Delta^2)^2}{\Delta^2} \right] \int_{-\frac{1}{\sqrt{2}} \ln \frac{4}{3}}^{\frac{1}{\sqrt{2}} \ln \frac{3}{2}} ds e^{-2\sqrt{2}s} (1 - 2e^{\sqrt{2}s})^2 \text{arcsinh} \left(\frac{e^{-s/\sqrt{2}}}{2} \right).\end{aligned}\quad (32)$$

In the second step, we have approximated the error function by taking the leading order at $\xi(s) \ll \sqrt{2}\Delta$. We have also approximated the Gaussian function in the integrand by putting s to its maximum value, $s = -(1/\sqrt{2})\ln(4/3)$. In passing, we note that Δ is assumed to be larger than the interval of the integral, $(1/\sqrt{2})\ln 2 \sim 0.49$, which corresponds to the critical width that separates the *narrow* and *broad* peaks. The integral in the second line of (32) gives a constant. Although it may be evaluated analytically, since the expression is very long and it is not illuminating, we do not spell it out here. Instead we simply quote its numerical value:

$$\Omega_{\text{GW,r}}^{|s|<1} \approx 0.0659 \frac{\mathcal{A}_{\mathcal{R}}^2}{\Delta^2} \kappa^2 e^{\Delta^2} \exp \left[-\frac{(\ln \kappa + \Delta^2 - \frac{1}{2} \ln \frac{4}{3})^2}{\Delta^2} \right]. \quad (33)$$

For $s \lesssim -1$, the domain of integration has two strips at the leftmost region of Fig. 1. Along both strips, we may assume $|s| \approx |t| \gg 1$, and the leading order of $\mathcal{T}(s, t)$ is given by

$$\mathcal{T}(s, t) = \frac{e^{4\sqrt{2}s}}{9}. \quad (34)$$

Then the integral along the t -axis is straightforward to find

$$2 \int_{\chi(s)}^{\xi(s)} \mathcal{T}(s, t) \exp \left(-\frac{t^2}{2\Delta^2} \right) dt \approx \frac{\sqrt{2\pi}}{9} e^{4\sqrt{2}s} \Delta \left(\text{erf} \left(\frac{\xi(s)}{\sqrt{2}\Delta} \right) - \text{erf} \left(\frac{\chi(s)}{\sqrt{2}\Delta} \right) \right) \approx \frac{4}{9} \sqrt{2} \exp \left(-\frac{s^2}{2\Delta^2} + 5\sqrt{2}s \right). \quad (35)$$

Substituting (35) into (15) and performing the Gaussian integral, we obtain

$$\begin{aligned}\Omega_{\text{GW,r}}^{s \lesssim -1} &\approx \frac{2\sqrt{2}}{3\pi} \mathcal{A}_{\mathcal{R}}^2 \kappa^{-4} \frac{e^{8\Delta^2}}{\Delta^2} \exp \left(-\frac{\ln^2 \kappa}{2\Delta^2} \right) \int_{-\infty}^{-\sqrt{2}\ln 2} \exp \left(-\frac{(s + \frac{1}{\sqrt{2}}(\ln \kappa - 4\Delta^2))^2}{\Delta^2} \right) ds, \\ &= \frac{1}{3} \sqrt{\frac{2}{\pi}} \mathcal{A}_{\mathcal{R}}^2 \kappa^{-4} \frac{e^{8\Delta^2}}{\Delta} \exp \left(-\frac{\ln^2 \kappa}{2\Delta^2} \right) \text{erfc} \left(\frac{4\Delta^2 - \ln(\kappa/4)}{\sqrt{2}\Delta} \right).\end{aligned}\quad (36)$$

This expression can be further simplified by using the asymptotic behavior of the complementary error function.

For $\kappa < 4e^{4\Delta^2}$, which includes the near-peak region of $\kappa \sim 1$, we find

$$\Omega_{\text{GW,r}}^{\text{(peak, } s < -1)} \approx \frac{1}{384\pi (4\Delta^2 - \ln(\kappa/4))} \exp \left(-\frac{\ln^2 \kappa + 2\ln^2 2}{\Delta^2} \right) \kappa^{\ln 4/\Delta^2} \approx \frac{\kappa^{\frac{\ln(4)}{\Delta^2}}}{1536\pi \Delta^2} \exp \left(-\frac{\ln^2(\kappa)}{\Delta^2} \right). \quad (37)$$

We see that the coefficient is much smaller than those of (30) and (33), which constitute the near-peak contributions from $s > 1$ and $|s| < 1$, respectively. So we conclude that (37) is negligible around the peak, and reach a pretty good approximate near-peak formula as a sum of (30) and (33),

$$\Omega_{\text{GW,r}}^{\text{(near-peak)}} \approx 0.0676 \frac{\mathcal{A}_{\mathcal{R}}^2}{\Delta^2} \frac{e^{9\Delta^2/4}}{\Delta^2} \exp \left(-\frac{(\ln \kappa + \frac{3}{2}\Delta^2 + \frac{1}{2} \ln \frac{3}{2})^2}{\Delta^2} \right) + 0.0659 \frac{\mathcal{A}_{\mathcal{R}}^2}{\Delta^2} \kappa^2 e^{\Delta^2} \exp \left[-\frac{(\ln \kappa + \Delta^2 - \frac{1}{2} \ln \frac{4}{3})^2}{\Delta^2} \right], \quad (38)$$

where we have calculated the numerical factor in (30).

For $\kappa > 4e^{4\Delta^2}$, the complementary error function gives a constant of 2, hence

$$\Omega_{\text{GW,r}}^{\text{(UV, } s < -1)} \approx \frac{2}{3} \sqrt{\frac{2}{\pi}} \mathcal{A}_{\mathcal{R}}^2 \kappa^{-4} \frac{e^{8\Delta^2}}{\Delta} \exp \left(-\frac{\ln^2 \kappa}{2\Delta^2} \right). \quad (39)$$

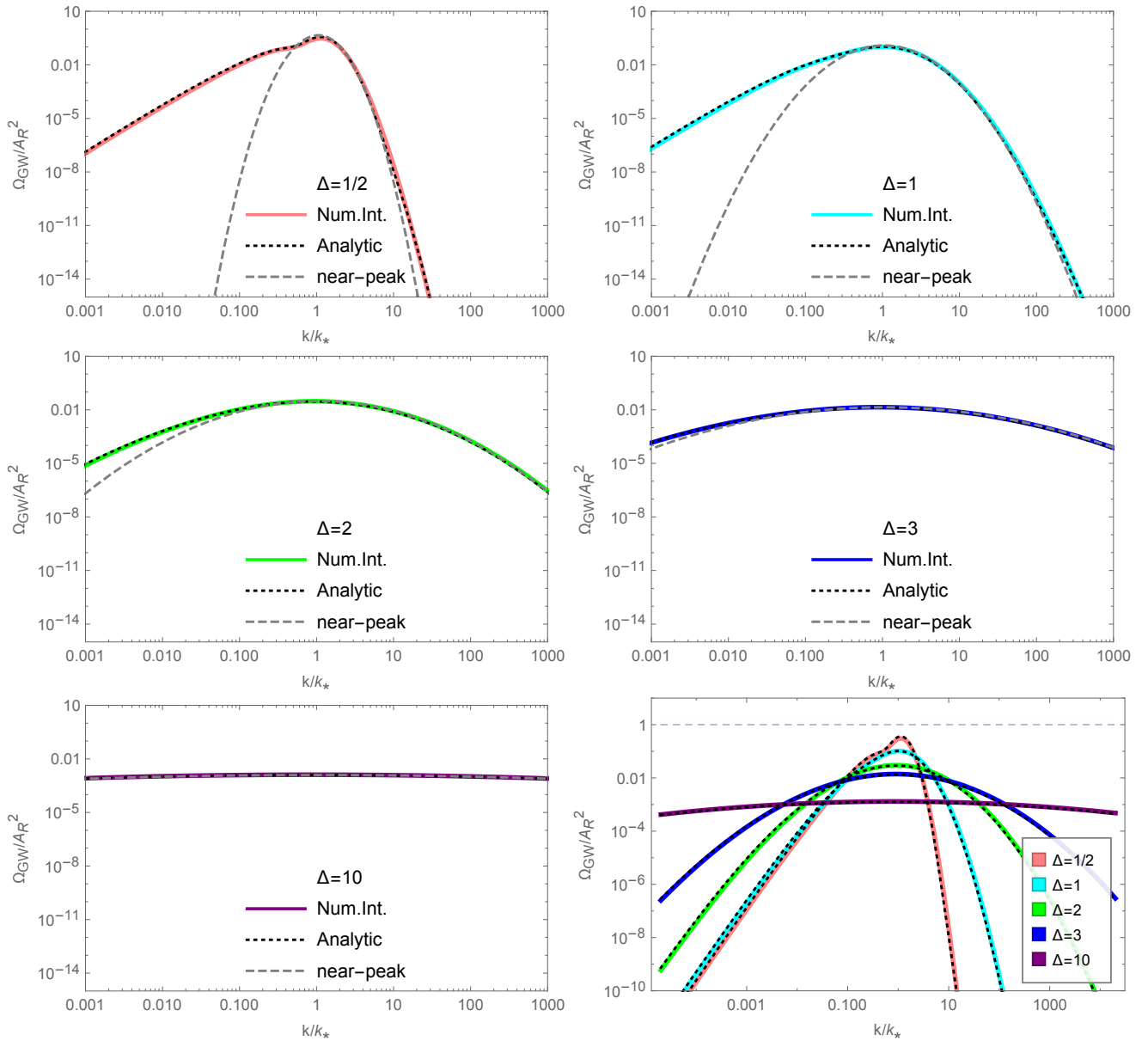


FIG. 3: The GW spectra for $\Delta = 1/2$ (top left), $\Delta = 1$ (top right), $\Delta = 2$ (middle left), $\Delta = 3$ (middle right), and $\Delta = 10$ (bottom left), respectively. The solid thick curves are the results by numerical integration of (13). The black dotted curves are the approximate analytical expressions (40). The near-peak approximation (38) is also shown as gray dashed curves. The GW spectra for different widths are drawn together in the bottom right panel for comparison. A double-peak structure in the narrow-peak case is barely seen in the case $\Delta = 1/2$, which is slightly above the critical value that divides narrow and broad peaks, $\Delta = \Delta_c \sim 0.4$.

This overwhelms the contributions given by (28) and (33), and gives an approximate expression of $\Omega_{\text{GW},r}$ in the ultraviolet region. But we have to keep in mind that this “ultraviolet” region is far away from the peak when $\Delta \gtrsim 1$, and, because of the exponential suppression, it is probably too difficult to be detected.

To summarize, the final result of the GW spectrum when $\Delta \gtrsim \mathcal{O}(1)$ is the summation of (28), (33), and (36):

$$\begin{aligned} \frac{\Omega_{\text{GW,r}}}{\mathcal{A}_{\mathcal{R}}^2} &\approx \frac{4}{5\sqrt{\pi}} \kappa^3 \frac{e^{\frac{9\Delta^2}{4}}}{\Delta} \left[\left(\ln^2 K + \frac{\Delta^2}{2} \right) \text{erfc} \left(\frac{\ln K + \frac{1}{2} \ln \frac{3}{2}}{\Delta} \right) - \frac{\Delta}{\sqrt{\pi}} \exp \left(-\frac{(\ln K + \frac{1}{2} \ln \frac{3}{2})^2}{\Delta^2} \right) \left(\ln K - \frac{1}{2} \ln \frac{3}{2} \right) \right] \\ &+ \frac{0.0659}{\Delta^2} \kappa^2 e^{\Delta^2} \exp \left(-\frac{(\ln \kappa + \Delta^2 - \frac{1}{2} \ln \frac{4}{3})^2}{\Delta^2} \right) + \frac{1}{3} \sqrt{\frac{2}{\pi}} \kappa^{-4} \frac{e^{8\Delta^2}}{\Delta} \exp \left(-\frac{\ln^2 \kappa}{2\Delta^2} \right) \text{erfc} \left(\frac{4\Delta^2 - \ln(\kappa/4)}{\sqrt{2}\Delta} \right), \end{aligned} \quad (40)$$

where we have introduced $K = \kappa \exp(3\Delta^2/2)$ for simplicity. This is one of the main results of this paper. Its accuracy can be checked by looking at Fig. 3 where the numerical results are also shown. It is also useful to write down the asymptotic expressions of (29), (38), and (39), each of which gives the GW spectrum valid in each different region,

$$\frac{\Omega_{\text{GW,r}}}{\mathcal{A}_{\mathcal{R}}^2} \approx \begin{cases} \frac{3}{\sqrt{\pi}} \frac{e^{\frac{9\Delta^2}{4}}}{\Delta} \kappa^3 \left[\left(\ln \kappa + \frac{3}{2} \Delta^2 \right)^2 + \frac{\Delta^2}{2} \right], & \text{for } \kappa \ll \sqrt{\frac{2}{3}} e^{-\frac{3}{2}\Delta^2}; \quad (\text{infrared}) \\ \frac{0.125}{\Delta^2} \exp \left(-\frac{\ln^2 \kappa}{\Delta^2} \right), & \text{for } \sqrt{\frac{2}{3}} e^{-\frac{3}{2}\Delta^2} \ll \kappa \ll 4e^{4\Delta^2}; \quad (\text{near peak}) \\ \frac{2}{3} \sqrt{\frac{2}{\pi}} \kappa^{-4} \frac{e^{8\Delta^2}}{\Delta} \exp \left(-\frac{\ln^2 \kappa}{2\Delta^2} \right), & \text{for } \kappa \gg 4e^{4\Delta^2}. \quad (\text{ultraviolet}) \end{cases} \quad (41)$$

Although each of the above asymptotic formula fits very well in each region, we only plot the most important, near-peak formula in Fig. 3, which is (38). When $\Delta \gtrsim 1$, it can be further simplified as

$$\Omega_{\text{GW,r}}^{(\text{peak})} \approx 0.125 \frac{\mathcal{A}_{\mathcal{R}}^2}{\Delta^2} \exp \left(-\frac{\ln^2 \kappa}{\Delta^2} \right). \quad (42)$$

This formula for the near-peak region is another main result of this paper. It clearly shows that the induced GW spectrum has a lognormal peak with width $\Delta/\sqrt{2}$ which is smaller by $\sqrt{2}$ of the peak width of the original curvature perturbation spectrum, Δ . This is a reflection of the ‘‘secondary’’ nature of the induced GWs, as $\Omega_{\text{GW,r}} \propto (\mathcal{P}_{\mathcal{R}})^2$.[¶] The maximum of the GW spectrum is given directly by setting $\kappa = 1$,

$$\Omega_{\text{GW,r}}^{(\text{max})} \approx 0.125 \frac{\mathcal{A}_{\mathcal{R}}^2}{\Delta^2}. \quad (43)$$

Since (42) gives the height and width of the peak of the induced GW spectrum, we expect it to play an important role in the interpretation of observational signals in the near future.

An important special case of a broad peak is the GWs induced by a scale-invariant curvature perturbation, $\mathcal{P}_{\mathcal{R}}(k) = A_{\mathcal{R}}$. Comparing to (12), this corresponds to the limits $\mathcal{A}_{\mathcal{R}} \rightarrow \infty$ and $\Delta \rightarrow \infty$ with the ratio $\mathcal{A}_{\mathcal{R}}/(\sqrt{2\pi}\Delta) \equiv A_{\mathcal{R}} = \text{const.}$. This gives a scale-invariant GW spectrum,

$$\Omega_{\text{GW,r}} = 0.783 A_{\mathcal{R}}^2, \quad (44)$$

which is in good agreement with the result obtained numerically in Ref. [17].

IV. CONCLUSION

In this expanding new era of GW astronomy/cosmology, detecting the stochastic background of GWs is the next scientific goal for the GW experiments in the coming decades. Among possible sources of stochastic backgrounds, the secondary GWs induced by the primordial curvature perturbation is a very important target. As both the generation of GWs and the formation of PBHs occur essentially at the horizon reentry of the relevant scale in the early universe, the fruitful PBH physics motivated us to study the associated induced GWs. Observations on both sides can be used to probe the primordial curvature perturbation on small scales, where there is no stringent constraints.

[¶]We thank Rong-Gen Cai for pointing out this simple physical explanation for the relation between the two widths.

In this paper we have studied the spectrum of GWs induced by the primordial curvature perturbation whose spectrum has a lognormal peak. Such a spectrum is frequently discussed in the literature from the viewpoints of both inflationary phenomenology and PBH formation mechanism. We have found that the resulting spectrum of the induced GWs has distinct features depending on the width of the lognormal spectrum, Δ . For both narrow-peak ($\Delta \ll 1$) and broad-peak ($\Delta \gtrsim 1$) cases, we have successfully obtained an analytical formula with amazingly good accuracy, as presented in (19) for $\Delta \ll 1$ and (40) for $\Delta \gtrsim 1$, respectively.

For the narrow-peak case, the GW spectrum (19) can be further simplified by using the GW spectrum for a δ -function peak. Namely, it may be factorized into two components,

$$\Omega_{\text{GW},r}^{(\Delta \ll 1)} \approx \text{erf} \left(\frac{1}{\Delta} \text{arcsinh} \frac{k}{2k_*} \right) \Omega_{\text{GW},r}^{(\delta)}, \quad (45)$$

where the factor given by the error function is independent of the equation of state of the universe, and $\Omega_{\text{GW},r}^{(\delta)}$ is for the δ -function curvature perturbation spectrum whose formula in the radiation-dominated universe, (20), is well known, and it is not difficult to extend it to that for a universe with arbitrary equation of state. Thus (45) gives a universal formula valid for any equation of state of the universe if $\Delta \ll 1$.

As $\Omega_{\text{GW},r}^{(\delta)} \propto k^2$ in the radiation dominated universe, (45) clearly shows there is a break in the power-law at $k_b \approx 2k_*\Delta$ on the infrared side of the GW spectrum, changing from k^3 to k^2 as k increases. In addition, there appears a logarithmically diverging peak at $k_p \approx 2k_*/\sqrt{3}$. If such a GW spectrum is observed in the future, with both break and peak frequencies measured, the width of the peak in the original curvature perturbation spectrum can be read off as

$$\Delta \approx \frac{f_b}{\sqrt{3}f_p}, \quad (46)$$

where f_b and f_p are the break and peak frequencies, respectively.

For the broad-peak case, we have also derived an analytical expression (40) which fits the numerical result very well. Further, we have obtained the asymptotic expressions for infrared, near-peak, and ultraviolet regions, respectively. The most important feature of the GW spectrum for the broad-peak case is the appearance of a lognormal peak with width $\Delta/\sqrt{2}$, which is smaller by $\sqrt{2}$ compared with the width Δ of the primordial curvature perturbation, as shown in (42), which reflects the secondary nature of the induced GWs.

The maximum of the GW spectrum has been also derived,

$$\frac{\Omega_{\text{GW},r}^{(\text{max})}}{\mathcal{A}_{\mathcal{R}}^2} = \begin{cases} \frac{4}{9} \left(\ln(2\Delta) + 1 \right)^2 + 2.64 & \text{for } \delta f < \Delta \ll 1, \\ \frac{0.125}{\Delta^2} & \text{for } \Delta \gtrsim 1. \end{cases} \quad (47)$$

As we stated at the end of Section II, all the results of $\Omega_{\text{GW},r}$ listed above are valid only until the epoch of matter-radiation equality. To obtain the GW spectrum we observe today, they should be multiplied by a redshift factor of $2\Omega_{r,0} \sim 8.2 \times 10^{-5}$.

In this paper we have only considered lognormal spectra for the primordial curvature perturbation. Such spectra may arise in varieties of inflation models, which implies the usefulness of our results. Nevertheless, the primordial curvature perturbation may have a more complicated spectrum. For example, the spectrum may be composed of Gaussian fluctuations and non-Gaussian corrections. In such a case, even if the Gaussian part has a lognormal spectrum, the non-Gaussian part may substantially deform the spectral shape if its contribution is large. A specific example was discussed in Ref. [18] where the local-type non-Gaussianity is added on top of the Gaussian perturbation: $\mathcal{R} = \mathcal{R}_g + F_{\text{NL}} (\mathcal{R}_g^2 - \langle \mathcal{R}_g^2 \rangle)$ with a narrowly peaked spectrum of \mathcal{R}_g . Deriving analytical expressions for more general forms of the primordial curvature perturbation spectrum is a challenging issue left for future work.

Acknowledgments

We thank Rong-Gen Cai and Guillem Domènech for useful discussions. S.P. especially thanks his father Tian-Ming Pi for taking care of him when he was working in his hometown under the lockdown in Hubei Province, China during the COVID-19 pandemic. The work of S.P. is supported in part by JSPS Grant-in-Aid for Early-Career Scientists No. 20K14461. The work of M.S. is supported in part by the JSPS KAKENHI Nos. 19H01895 and 20H04727. Both

S.P. and M.S. are supported by the World Premier International Research Center Initiative (WPI Initiative), MEXT, Japan.

-
- [1] B. P. Abbott *et al.* [LIGO Scientific and Virgo Collaborations], Phys. Rev. Lett. **116**, no. 6, 061102 (2016) doi:10.1103/PhysRevLett.116.061102 [arXiv:1602.03837 [gr-qc]]. B. P. Abbott *et al.* [LIGO Scientific and Virgo Collaborations], Phys. Rev. Lett. **116**, no. 24, 241103 (2016) doi:10.1103/PhysRevLett.116.241103 [arXiv:1606.04855 [gr-qc]]. B. P. Abbott *et al.* [LIGO Scientific and VIRGO Collaborations], Phys. Rev. Lett. **118**, no. 22, 221101 (2017) doi:10.1103/PhysRevLett.118.221101 [arXiv:1706.01812 [gr-qc]]. B. P. Abbott *et al.* [LIGO Scientific and Virgo Collaborations], Astrophys. J. **851**, no. 2, L35 (2017) doi:10.3847/2041-8213/aa9f0c [arXiv:1711.05578 [astro-ph.HE]]. B. P. Abbott *et al.* [LIGO Scientific and Virgo Collaborations], Phys. Rev. Lett. **119**, no. 14, 141101 (2017) doi:10.1103/PhysRevLett.119.141101 [arXiv:1709.09660 [gr-qc]]. B. P. Abbott *et al.* [LIGO Scientific and Virgo Collaborations], “GW170817: Observation of Gravitational Waves from a Binary Neutron Star Inspiral,” Phys. Rev. Lett. **119**, no. 16, 161101 (2017) doi:10.1103/PhysRevLett.119.161101 [arXiv:1710.05832 [gr-qc]]. B. P. Abbott *et al.* [LIGO Scientific and Virgo Collaborations], arXiv:2001.01761 [astro-ph.HE].
- [2] S. Matarrese, O. Pantano and D. Saez, Phys. Rev. D **47**, 1311 (1993). S. Matarrese, O. Pantano and D. Saez, Phys. Rev. Lett. **72**, 320 (1994) [astro-ph/9310036]. S. Matarrese, S. Mollerach and M. Bruni, Phys. Rev. D **58**, 043504 (1998) [astro-ph/9707278]. H. Noh and J. c. Hwang, Phys. Rev. D **69** (2004) 104011. C. Carbone and S. Matarrese, Phys. Rev. D **71** (2005) 043508 [astro-ph/0407611]. K. Nakamura, Prog. Theor. Phys. **117**, 17 (2007) [gr-qc/0605108].
- [3] D. Baumann, P. J. Steinhardt, K. Takahashi and K. Ichiki, Phys. Rev. D **76**, 084019 (2007) doi:10.1103/PhysRevD.76.084019 [hep-th/0703290].
- [4] K. N. Ananda, C. Clarkson and D. Wands, Phys. Rev. D **75**, 123518 (2007) doi:10.1103/PhysRevD.75.123518 [gr-qc/0612013].
- [5] B. Osano, C. Pitrou, P. Dunsby, J. P. Uzan and C. Clarkson, JCAP **0704**, 003 (2007) doi:10.1088/1475-7516/2007/04/003 [gr-qc/0612108].
- [6] R. Saito and J. Yokoyama, Phys. Rev. Lett. **102**, 161101 (2009) Erratum: [Phys. Rev. Lett. **107**, 069901 (2011)] doi:10.1103/PhysRevLett.102.161101, 10.1103/PhysRevLett.107.069901 [arXiv:0812.4339 [astro-ph]].
- [7] H. Assadullahi and D. Wands, Phys. Rev. D **79**, 083511 (2009) doi:10.1103/PhysRevD.79.083511 [arXiv:0901.0989 [astro-ph.CO]].
- [8] H. Assadullahi and D. Wands, Phys. Rev. D **81**, 023527 (2010) doi:10.1103/PhysRevD.81.023527 [arXiv:0907.4073 [astro-ph.CO]].
- [9] E. Bugaev and P. Klimai, Phys. Rev. D **81**, 023517 (2010) doi:10.1103/PhysRevD.81.023517 [arXiv:0908.0664 [astro-ph.CO]].
- [10] R. Saito and J. Yokoyama, Prog. Theor. Phys. **123**, 867 (2010) Erratum: [Prog. Theor. Phys. **126**, 351 (2011)] doi:10.1143/PTP.126.351, 10.1143/PTP.123.867 [arXiv:0912.5317 [astro-ph.CO]].
- [11] E. Bugaev and P. Klimai, Phys. Rev. D **83**, 083521 (2011) doi:10.1103/PhysRevD.83.083521 [arXiv:1012.4697 [astro-ph.CO]].
- [12] L. Alabidi, K. Kohri, M. Sasaki and Y. Sendouda, JCAP **1209**, 017 (2012) doi:10.1088/1475-7516/2012/09/017 [arXiv:1203.4663 [astro-ph.CO]].
- [13] L. Alabidi, K. Kohri, M. Sasaki and Y. Sendouda, JCAP **1305**, 033 (2013) [arXiv:1303.4519 [astro-ph.CO]].
- [14] T. Nakama, J. Silk and M. Kamionkowski, Phys. Rev. D **95** (2017) no.4, 043511 doi:10.1103/PhysRevD.95.043511 [arXiv:1612.06264 [astro-ph.CO]].
- [15] H. Di and Y. Gong, JCAP **1807**, no. 07, 007 (2018) doi:10.1088/1475-7516/2018/07/007 [arXiv:1707.09578 [astro-ph.CO]].
- [16] J. R. Espinosa, D. Racco and A. Riotto, JCAP **1809** (2018) no.09, 012 doi:10.1088/1475-7516/2018/09/012 [arXiv:1804.07732 [hep-ph]].
- [17] K. Kohri and T. Terada, Phys. Rev. D **97**, 123532 (2018) doi:10.1103/PhysRevD.97.123532 [arXiv:1804.08577 [gr-qc]].
- [18] R. g. Cai, S. Pi and M. Sasaki, Phys. Rev. Lett. **122**, no. 20, 201101 (2019) doi:10.1103/PhysRevLett.122.201101 [arXiv:1810.11000 [astro-ph.CO]].
- [19] N. Bartolo, V. De Luca, G. Franciolini, A. Lewis, M. Peloso and A. Riotto, Phys. Rev. Lett. **122**, no. 21, 211301 (2019) doi:10.1103/PhysRevLett.122.211301 [arXiv:1810.12218 [astro-ph.CO]].
- [20] N. Bartolo, V. De Luca, G. Franciolini, M. Peloso, D. Racco and A. Riotto, Phys. Rev. D **99**, no. 10, 103521 (2019) doi:10.1103/PhysRevD.99.103521 [arXiv:1810.12224 [astro-ph.CO]].
- [21] C. Unal, Phys. Rev. D **99**, no. 4, 041301 (2019) doi:10.1103/PhysRevD.99.041301 [arXiv:1811.09151 [astro-ph.CO]].
- [22] R. G. Cai, S. Pi, S. J. Wang and X. Y. Yang, JCAP **1905**, no. 05, 013 (2019) doi:10.1088/1475-7516/2019/05/013 [arXiv:1901.10152 [astro-ph.CO]].
- [23] C. Yuan, Z. C. Chen and Q. G. Huang, Phys. Rev. D **100**, no. 8, 081301 (2019) doi:10.1103/PhysRevD.100.081301 [arXiv:1906.11549 [astro-ph.CO]].
- [24] K. Inomata, K. Kohri, T. Nakama and T. Terada, arXiv:1904.12878 [astro-ph.CO].
- [25] K. Inomata, K. Kohri, T. Nakama and T. Terada, Phys. Rev. D **100**, no. 4, 043532 (2019) doi:10.1103/PhysRevD.100.043532 [arXiv:1904.12879 [astro-ph.CO]].
- [26] J. O. Gong, arXiv:1909.12708 [gr-qc].

- [27] A. Ota, Phys. Rev. D **101**, no. 10, 103511 (2020) doi:10.1103/PhysRevD.101.103511 [arXiv:2001.00409 [astro-ph.CO]].
- [28] K. Inomata, M. Kawasaki, K. Mukaida, T. Terada and T. T. Yanagida, arXiv:2003.10455 [astro-ph.CO].
- [29] N. Aghanim *et al.* [Planck Collaboration], arXiv:1807.06209 [astro-ph.CO].
- [30] Y. Watanabe and E. Komatsu, Phys. Rev. D **73**, 123515 (2006) doi:10.1103/PhysRevD.73.123515 [astro-ph/0604176].
- [31] S. Pi, M. Sasaki and Y. I. Zhang, JCAP **1906**, 049 (2019) doi:10.1088/1475-7516/2019/06/049 [arXiv:1904.06304 [gr-qc]].
- [32] C. T. Byrnes, P. S. Cole and S. P. Patil, arXiv:1811.11158 [astro-ph.CO].
- [33] K. Inomata and T. Nakama, Phys. Rev. D **99**, no. 4, 043511 (2019) doi:10.1103/PhysRevD.99.043511 [arXiv:1812.00674 [astro-ph.CO]].
- [34] I. Dalianis, arXiv:1812.09807 [astro-ph.CO]. Y. Lu, Y. Gong, Z. Yi and F. Zhang, JCAP **1912**, 031 (2019) doi:10.1088/1475-7516/2019/12/031 [arXiv:1907.11896 [gr-qc]]. A. Kalaja, N. Bellomo, N. Bartolo, D. Bertacca, S. Matarrese, I. Musco, A. Raccanelli and L. Verde, JCAP **1910**, 031 (2019) doi:10.1088/1475-7516/2019/10/031 [arXiv:1908.03596 [astro-ph.CO]]. O. zsoy and G. Tasinato, JCAP **2004**, 048 (2020) doi:10.1088/1475-7516/2020/04/048 [arXiv:1912.01061 [astro-ph.CO]].
- [35] Ya. B. Zel'dovich and I.D. Novikov, Sov. Astron. **10**, 602 (1966). S. Hawking, Mon. Not. Roy. Astron. Soc. **152**, 75 (1971). B. J. Carr and S. W. Hawking, Mon. Not. Roy. Astron. Soc. **168**, 399 (1974). P. Meszaros, Astron. Astrophys. **37**, 225 (1974). B. J. Carr, Astrophys. J. **201**, 1 (1975). M. Khlopov, B. A. Malomed and I. B. Zeldovich, Mon. Not. Roy. Astron. Soc. **215**, 575 (1985).
- [36] S. Young, C. T. Byrnes and M. Sasaki, JCAP **1407**, 045 (2014) doi:10.1088/1475-7516/2014/07/045 [arXiv:1405.7023 [gr-qc]]. C. Germani and I. Musco, Phys. Rev. Lett. **122**, no. 14, 141302 (2019) doi:10.1103/PhysRevLett.122.141302 [arXiv:1805.04087 [astro-ph.CO]]. V. De Luca, G. Franciolini, A. Kehagias, M. Peloso, A. Riotto and C. nal, JCAP **1907**, 048 (2019) doi:10.1088/1475-7516/2019/07/048 [arXiv:1904.00970 [astro-ph.CO]]. J. M. Ezquiaga, J. Garca-Bellido and V. Vennin, JCAP **2003**, 029 (2020) doi:10.1088/1475-7516/2020/03/029 [arXiv:1912.05399 [astro-ph.CO]]. Y. P. Wu, arXiv:2005.00441 [astro-ph.CO].
- [37] A. M. Green, A. R. Liddle, K. A. Malik and M. Sasaki, Phys. Rev. D **70**, 041502 (2004) [astro-ph/0403181]. P. Tisserand *et al.* [EROS-2 Collaboration], Astron. Astrophys. **469**, 387 (2007) doi:10.1051/0004-6361:20066017 [astro-ph/0607207]. P. H. Frampton, JCAP **0910**, 016 (2009) [arXiv:0905.3632 [hep-th]]. B. J. Carr, K. Kohri, Y. Sendouda and J. Yokoyama, Phys. Rev. D **81**, 104019 (2010) [arXiv:0912.5297 [astro-ph.CO]]. P. W. Graham, S. Rajendran and J. Varela, Phys. Rev. D **92**, no. 6, 063007 (2015) doi:10.1103/PhysRevD.92.063007 [arXiv:1505.04444 [hep-ph]]. B. J. Carr, K. Kohri, Y. Sendouda and J. Yokoyama, Phys. Rev. D **94**, no. 4, 044029 (2016) doi:10.1103/PhysRevD.94.044029 [arXiv:1604.05349 [astro-ph.CO]]. B. Carr, F. Kuhnel and M. Sandstad, Phys. Rev. D **94**, no. 8, 083504 (2016) [arXiv:1607.06077 [astro-ph.CO]]. S. M. Koushiappas and A. Loeb, Phys. Rev. Lett. **119**, no. 4, 041102 (2017) doi:10.1103/PhysRevLett.119.041102 [arXiv:1704.01668 [astro-ph.GA]]. S. Wang, T. Terada and K. Kohri, Phys. Rev. D **99**, no. 10, 103531 (2019) doi:10.1103/PhysRevD.99.103531 [arXiv:1903.05924 [astro-ph.CO]]. B. P. Abbott *et al.* [LIGO Scientific and Virgo Collaborations], Phys. Rev. Lett. **123**, no. 16, 161102 (2019) doi:10.1103/PhysRevLett.123.161102 [arXiv:1904.08976 [astro-ph.CO]]. H. Poulter, Y. Ali-Hamoud, J. Hamann, M. White and A. G. Williams, arXiv:1907.06485 [astro-ph.CO]. P. D. Serpico, V. Poulin, D. Inman and K. Kohri, arXiv:2002.10771 [astro-ph.CO]. V. De Luca, G. Franciolini, P. Pani and A. Riotto, arXiv:2005.05641 [astro-ph.CO].
- [38] S. Bird, I. Cholis, J. B. Muñoz, Y. Ali-Haimoud, M. Kamionkowski, E. D. Kovetz, A. Raccanelli and A. G. Riess, Phys. Rev. Lett. **116**, no. 20, 201301 (2016) [arXiv:1603.00464 [astro-ph.CO]]. S. Clesse and J. Garcia-Bellido, Phys. Dark Univ. **15**, 142 (2017) [arXiv:1603.05234 [astro-ph.CO]]. M. Sasaki, T. Suyama, T. Tanaka and S. Yokoyama, Phys. Rev. Lett. **117**, no. 6, 061101 (2016) [arXiv:1603.08338 [astro-ph.CO]]. L. Chen, Q. G. Huang and K. Wang, JCAP **1612**, no. 12, 044 (2016) [arXiv:1608.02174 [astro-ph.CO]]. S. Blinnikov, A. Dolgov, N. K. Porayko and K. Postnov, JCAP **1611**, no. 11, 036 (2016) [arXiv:1611.00541 [astro-ph.HE]]. Y. Ali-Haimoud and M. Kamionkowski, Phys. Rev. D **95**, no. 4, 043534 (2017) [arXiv:1612.05644 [astro-ph.CO]]. M. Zumalacarregui and U. Seljak, Phys. Rev. Lett. **121**, no. 14, 141101 (2018) doi:10.1103/PhysRevLett.121.141101 [arXiv:1712.02240 [astro-ph.CO]]. J. Garcia-Bellido, S. Clesse and P. Fleury, Phys. Dark Univ. **20**, 95 (2018) doi:10.1016/j.dark.2018.04.005 [arXiv:1712.06574 [astro-ph.CO]].
- [39] H. Niikura *et al.*, Nat. Astron. **3**, no. 6, 524 (2019) doi:10.1038/s41550-019-0723-1 [arXiv:1701.02151 [astro-ph.CO]]. A. Katz, J. Kopp, S. Sibiryakov and W. Xue, JCAP **1812**, 005 (2018) doi:10.1088/1475-7516/2018/12/005 [arXiv:1807.11495 [astro-ph.CO]]. P. Montero-Camacho, X. Fang, G. Vasquez, M. Silva and C. M. Hirata, JCAP **1908**, 031 (2019) doi:10.1088/1475-7516/2019/08/031 [arXiv:1906.05950 [astro-ph.CO]]. S. Sugiyama, T. Kurita and M. Takada, doi:10.1093/mnras/staa407 arXiv:1905.06066 [astro-ph.CO]. W. DeRocco and P. W. Graham, Phys. Rev. Lett. **123**, no. 25, 251102 (2019) doi:10.1103/PhysRevLett.123.251102 [arXiv:1906.07740 [astro-ph.CO]]. R. Laha, Phys. Rev. Lett. **123**, no. 25, 251101 (2019) doi:10.1103/PhysRevLett.123.251101 [arXiv:1906.09994 [astro-ph.HE]].
- [40] R. Bean and J. Magueijo, Phys. Rev. D **66**, 063505 (2002) doi:10.1103/PhysRevD.66.063505 [astro-ph/0204486]. M. Kawasaki, A. Kusenko and T. T. Yanagida, Phys. Lett. B **711**, 1 (2012) doi:10.1016/j.physletb.2012.03.056 [arXiv:1202.3848 [astro-ph.CO]]. T. Nakama, B. Carr and J. Silk, Phys. Rev. D **97**, no. 4, 043525 (2018) doi:10.1103/PhysRevD.97.043525 [arXiv:1710.06945 [astro-ph.CO]]. B. Carr and J. Silk, Mon. Not. Roy. Astron. Soc. **478**, no. 3, 3756 (2018) doi:10.1093/mnras/sty1204 [arXiv:1801.00672 [astro-ph.CO]]. T. Nakama, K. Kohri and J. Silk, Phys. Rev. D **99**, no. 12, 123530 (2019) doi:10.1103/PhysRevD.99.123530 [arXiv:1905.04477 [astro-ph.CO]].
- [41] J. Scholtz and J. Unwin, arXiv:1909.11090 [hep-ph]. E. Witten, arXiv:2004.14192 [astro-ph.EP].
- [42] C. T. Byrnes, M. Hindmarsh, S. Young and M. R. S. Hawkins, JCAP **1808**, 041 (2018) doi:10.1088/1475-7516/2018/08/041 [arXiv:1801.06138 [astro-ph.CO]]. B. Carr, S. Clesse and J. Garca-Bellido, arXiv:1904.02129 [astro-ph.CO]. J. Garca-Bellido, B. Carr and S. Clesse, arXiv:1904.11482 [astro-ph.CO]. B. Carr, S. Clesse, J. Garcia-Bellido and F. Kuhnel, arXiv:1906.08217 [astro-ph.CO]. F. Hajkarim and J. Schaffner-Bielich, Phys. Rev. D **101**, no. 4, 043522

- (2020) doi:10.1103/PhysRevD.101.043522 [arXiv:1910.12357 [hep-ph]].
- [43] M. Sasaki, T. Suyama, T. Tanaka and S. Yokoyama, *Class. Quant. Grav.* **35**, no. 6, 063001 (2018) doi:10.1088/1361-6382/aaa7b4 [arXiv:1801.05235 [astro-ph.CO]].
- [44] B. Carr, K. Kohri, Y. Sendouda and J. Yokoyama, arXiv:2002.12778 [astro-ph.CO].
- [45] J. Yokoyama, *Phys. Rev. D* **58**, 083510 (1998) doi:10.1103/PhysRevD.58.083510 [astro-ph/9802357].
- [46] S. L. Cheng, W. Lee and K. W. Ng, *JHEP* **1702** (2017) 008 doi:10.1007/JHEP02(2017)008 [arXiv:1606.00206 [astro-ph.CO]].
- [47] J. Garcia-Bellido and E. Ruiz Morales, *Phys. Dark Univ.* **18**, 47 (2017) doi:10.1016/j.dark.2017.09.007 [arXiv:1702.03901 [astro-ph.CO]].
- [48] S. L. Cheng, W. Lee and K. W. Ng, *JCAP* **1807**, no. 07, 001 (2018) doi:10.1088/1475-7516/2018/07/001 [arXiv:1801.09050 [astro-ph.CO]].
- [49] I. Dalianis, A. Kehagias and G. Tringas, *JCAP* **1901**, 037 (2019) doi:10.1088/1475-7516/2019/01/037 [arXiv:1805.09483 [astro-ph.CO]].
- [50] T. J. Gao and Z. K. Guo, *Phys. Rev. D* **98**, no. 6, 063526 (2018) doi:10.1103/PhysRevD.98.063526 [arXiv:1806.09320 [hep-ph]].
- [51] Y. Tada and S. Yokoyama, *Phys. Rev. D* **100**, no. 2, 023537 (2019) doi:10.1103/PhysRevD.100.023537 [arXiv:1904.10298 [astro-ph.CO]].
- [52] W. T. Xu, J. Liu, T. J. Gao and Z. K. Guo, *Phys. Rev. D* **101**, no. 2, 023505 (2020) doi:10.1103/PhysRevD.101.023505 [arXiv:1907.05213 [astro-ph.CO]].
- [53] V. Atal, J. Cid, A. Escriv and J. Garriga, *JCAP* **2005**, 022 (2020) doi:10.1088/1475-7516/2020/05/022 [arXiv:1908.11357 [astro-ph.CO]].
- [54] S. S. Mishra and V. Sahni, *JCAP* **2004**, 007 (2020) doi:10.1088/1475-7516/2020/04/007 [arXiv:1911.00057 [gr-qc]].
- [55] J. Liu, Z. K. Guo and R. G. Cai, *Phys. Rev. D* **101**, no. 8, 083535 (2020) doi:10.1103/PhysRevD.101.083535 [arXiv:2003.02075 [astro-ph.CO]].
- [56] K. Kannike, L. Marzola, M. Raidal and H. Veermäe, *JCAP* **1709**, no. 09, 020 (2017) doi:10.1088/1475-7516/2017/09/020 [arXiv:1705.06225 [astro-ph.CO]].
- [57] S. Pi, Y. I. Zhang, Q. G. Huang and M. Sasaki, *JCAP* **1805**, no. 05, 042 (2018) doi:10.1088/1475-7516/2018/05/042 [arXiv:1712.09896 [astro-ph.CO]].
- [58] C. Fu, P. Wu and H. Yu, *Phys. Rev. D* **100**, no. 6, 063532 (2019) doi:10.1103/PhysRevD.100.063532 [arXiv:1907.05042 [astro-ph.CO]].
- [59] I. Dalianis, S. Karydas and E. Papantonopoulos, arXiv:1910.00622 [astro-ph.CO].
- [60] D. Y. Cheong, S. M. Lee and S. C. Park, arXiv:1912.12032 [hep-ph].
- [61] C. Fu, P. Wu and H. Yu, *Phys. Rev. D* **101**, no. 2, 023529 (2020) doi:10.1103/PhysRevD.101.023529 [arXiv:1912.05927 [astro-ph.CO]].
- [62] J. Lin, Q. Gao, Y. Gong, Y. Lu, C. Zhang and F. Zhang, arXiv:2001.05909 [gr-qc].
- [63] D. Y. Cheong, H. M. Lee and S. C. Park, doi:10.1016/j.physletb.2020.135453 arXiv:2002.07981 [hep-ph].
- [64] J. Garcia-Bellido, A. D. Linde and D. Wands, *Phys. Rev. D* **54**, 6040 (1996) doi:10.1103/PhysRevD.54.6040 [astro-ph/9605094].
- [65] M. Kawasaki, N. Sugiyama and T. Yanagida, *Phys. Rev. D* **57**, 6050 (1998) doi:10.1103/PhysRevD.57.6050 [hep-ph/9710259].
- [66] P. H. Frampton, M. Kawasaki, F. Takahashi and T. T. Yanagida, *JCAP* **1004**, 023 (2010) doi:10.1088/1475-7516/2010/04/023 [arXiv:1001.2308 [hep-ph]].
- [67] S. Clesse and J. Garcia-Bellido, *Phys. Rev. D* **92**, no. 2, 023524 (2015) doi:10.1103/PhysRevD.92.023524 [arXiv:1501.07565 [astro-ph.CO]].
- [68] K. Inomata, M. Kawasaki, K. Mukaida, Y. Tada and T. T. Yanagida, *Phys. Rev. D* **96**, no. 4, 043504 (2017) doi:10.1103/PhysRevD.96.043504 [arXiv:1701.02544 [astro-ph.CO]].
- [69] J. R. Espinosa, D. Racco and A. Riotto, *Phys. Rev. Lett.* **120**, no. 12, 121301 (2018), doi:10.1103/PhysRevLett.120.121301 [arXiv:1710.11196 [hep-ph]].
- [70] K. Inomata, M. Kawasaki, K. Mukaida and T. T. Yanagida, *Phys. Rev. D* **97**, no. 4, 043514 (2018) doi:10.1103/PhysRevD.97.043514 [arXiv:1711.06129 [astro-ph.CO]].
- [71] M. Kawasaki, H. Nakatsuka and I. Obata, *JCAP* **2005**, 007 (2020) doi:10.1088/1475-7516/2020/05/007 [arXiv:1912.09111 [astro-ph.CO]].
- [72] G. A. Palma, S. Sypsas and C. Zenteno, arXiv:2004.06106 [astro-ph.CO].
- [73] J. Fumagalli, S. Renaux-Petel, J. W. Ronayne and L. T. Witkowski, arXiv:2004.08369 [hep-th].
- [74] M. Braglia, D. K. Hazra, F. Finelli, G. F. Smoot, L. Sriramkumar and A. A. Starobinsky, arXiv:2005.02895 [astro-ph.CO].
- [75] M. Kawasaki, N. Kitajima and T. T. Yanagida, *Phys. Rev. D* **87**, no. 6, 063519 (2013) doi:10.1103/PhysRevD.87.063519 [arXiv:1207.2550 [hep-ph]].
- [76] K. Kohri, C. M. Lin and T. Matsuda, *Phys. Rev. D* **87**, no. 10, 103527 (2013) doi:10.1103/PhysRevD.87.103527 [arXiv:1211.2371 [hep-ph]].
- [77] K. Ando, K. Inomata, M. Kawasaki, K. Mukaida and T. T. Yanagida, *Phys. Rev. D* **97**, no. 12, 123512 (2018) doi:10.1103/PhysRevD.97.123512 [arXiv:1711.08956 [astro-ph.CO]].
- [78] K. Ando, M. Kawasaki and H. Nakatsuka, [arXiv:1805.07757 [astro-ph.CO]].
- [79] R. G. Cai, Z. K. Guo, J. Liu, L. Liu and X. Y. Yang, arXiv:1912.10437 [astro-ph.CO].

- [80] Y. F. Cai, X. Tong, D. G. Wang and S. F. Yan, Phys. Rev. Lett. **121**, no. 8, 081306 (2018) doi:10.1103/PhysRevLett.121.081306 [arXiv:1805.03639 [astro-ph.CO]].
- [81] Y. F. Cai, C. Chen, X. Tong, D. G. Wang and S. F. Yan, Phys. Rev. D **100**, no. 4, 043518 (2019) doi:10.1103/PhysRevD.100.043518 [arXiv:1902.08187 [astro-ph.CO]].
- [82] C. Chen and Y. F. Cai, JCAP **1910**, 068 (2019) doi:10.1088/1475-7516/2019/10/068 [arXiv:1908.03942 [astro-ph.CO]].
- [83] C. Chen, X. H. Ma and Y. F. Cai, arXiv:2003.03821 [astro-ph.CO].
- [84] K. Somiya [KAGRA Collaboration], Class. Quant. Grav. **29**, 124007 (2012) doi:10.1088/0264-9381/29/12/124007 [arXiv:1111.7185 [gr-qc]].
- [85] P. Amaro-Seoane *et al.*, GW Notes **6**, 4 (2013) [arXiv:1201.3621 [astro-ph.CO]]. P. Amaro-Seoane *et al.*, Class. Quant. Grav. **29**, 124016 (2012) doi:10.1088/0264-9381/29/12/124016 [arXiv:1202.0839 [gr-qc]]. H. Audley *et al.* [LISA Collaboration], arXiv:1702.00786 [astro-ph.IM]. E. Barausse *et al.*, doi:10.1007/s10714-020-02691-1. arXiv:2001.09793 [gr-qc].
- [86] Z. K. Guo, R. G. Cai and Y. Z. Zhang, arXiv:1807.09495 [gr-qc].
- [87] J. Luo *et al.* [TianQin Collaboration], Class. Quant. Grav. **33**, no. 3, 035010 (2016) doi:10.1088/0264-9381/33/3/035010 [arXiv:1512.02076 [astro-ph.IM]].
- [88] M. Punturo *et al.*, Class. Quant. Grav. **27**, 194002 (2010). doi:10.1088/0264-9381/27/19/194002 B. Sathyaprakash *et al.*, Class. Quant. Grav. **29**, 124013 (2012) Erratum: [Class. Quant. Grav. **30**, 079501 (2013)] doi:10.1088/0264-9381/29/12/124013, 10.1088/0264-9381/30/7/079501 [arXiv:1206.0331 [gr-qc]].
- [89] S. Kawamura *et al.*, Class. Quant. Grav. **28**, 094011 (2011). doi:10.1088/0264-9381/28/9/094011
- [90] J. Crowder and N. J. Cornish, Phys. Rev. D **72**, 083005 (2005) doi:10.1103/PhysRevD.72.083005 [gr-qc/0506015]. V. Corbin and N. J. Cornish, Class. Quant. Grav. **23**, 2435 (2006) doi:10.1088/0264-9381/23/7/014 [gr-qc/0512039]. J. Baker *et al.*, arXiv:1907.11305 [astro-ph.IM].
- [91] J. Lu, K. Lee and R. Xu, Sci. China Phys. Mech. Astron. **63**, no. 2, 229531 (2020) doi:10.1007/s11433-019-1453-2 [arXiv:1909.03707 [astro-ph.HE]].
- [92] G. Janssen *et al.*, PoS AASKA **14**, 037 (2015) doi:10.22323/1.215.0037 [arXiv:1501.00127 [astro-ph.IM]]. R. Maartens *et al.* [SKA Cosmology SWG Collaboration], PoS AASKA **14**, 016 (2015) doi:10.22323/1.215.0016 [arXiv:1501.04076 [astro-ph.CO]].
- [93] M. V. Sazhin, Vestn. Mosk. Univ. Fiz. Astron. **18**, no. 6, 82 (1977). S. L. Detweiler, Astrophys. J. **234**, 1100 (1979). doi:10.1086/157593
- [94] L. Lentati *et al.*, Mon. Not. Roy. Astron. Soc. **453**, no. 3, 2576 (2015) doi:10.1093/mnras/stv1538 [arXiv:1504.03692 [astro-ph.CO]]. K. Inomata, M. Kawasaki, K. Mukaida, Y. Tada and T. T. Yanagida, Phys. Rev. D **95**, no. 12, 123510 (2017) doi:10.1103/PhysRevD.95.123510 [arXiv:1611.06130 [astro-ph.CO]]. N. Orlofsky, A. Pierce and J. D. Wells, Phys. Rev. D **95**, no. 6, 063518 (2017) doi:10.1103/PhysRevD.95.063518 [arXiv:1612.05279 [astro-ph.CO]]. R. G. Cai, S. Pi, S. J. Wang and X. Y. Yang, JCAP **1910**, no. 10, 059 (2019) doi:10.1088/1475-7516/2019/10/059 [arXiv:1907.06372 [astro-ph.CO]]. Z. C. Chen, C. Yuan and Q. G. Huang, arXiv:1910.12239 [astro-ph.CO].
- [95] J. M. Bardeen, Phys. Rev. D **22**, 1882-1905 (1980) doi:10.1103/PhysRevD.22.1882
- [96] R. G. Cai, S. Pi and M. Sasaki, arXiv:1909.13728 [astro-ph.CO].
- [97] C. Yuan, Z. C. Chen and Q. G. Huang, Phys. Rev. D **101**, no. 4, 043019 (2020) doi:10.1103/PhysRevD.101.043019 [arXiv:1910.09099 [astro-ph.CO]].
- [98] J. T. Giblin and E. Thrane, Phys. Rev. D **90**, no. 10, 107502 (2014) doi:10.1103/PhysRevD.90.107502 [arXiv:1410.4779 [gr-qc]].
- [99] S. Bhattacharya, S. Mohanty and P. Parashari, arXiv:1912.01653 [astro-ph.CO].
- [100] G. Domènech, arXiv:1912.05583 [gr-qc].
- [101] G. Domènech, S. Pi and M. Sasaki, arXiv:2005.12314 [gr-qc].
- [102] K. Inomata and T. Terada, Phys. Rev. D **101**, no. 2, 023523 (2020) doi:10.1103/PhysRevD.101.023523 [arXiv:1912.00785 [gr-qc]].
- [103] K. Tomikawa and T. Kobayashi, Phys. Rev. D **101**, no. 8, 083529 (2020) doi:10.1103/PhysRevD.101.083529 [arXiv:1910.01880 [gr-qc]]. V. De Luca, G. Franciolini, A. Kehagias and A. Riotto, JCAP **2003**, no. 03, 014 (2020) doi:10.1088/1475-7516/2020/03/014 [arXiv:1911.09689 [gr-qc]]. C. Yuan, Z. C. Chen and Q. G. Huang, Phys. Rev. D **101**, no. 6, 063018 (2020) doi:10.1103/PhysRevD.101.063018 [arXiv:1912.00885 [astro-ph.CO]]. M. Giovannini, arXiv:2005.04962 [hep-th].
- [104] E. Thrane and J. D. Romano, Phys. Rev. D **88**, no. 12, 124032 (2013) doi:10.1103/PhysRevD.88.124032 [arXiv:1310.5300 [astro-ph.IM]].